ISSN: 0975 -8542

Journal of Global Pharma Technology

Available Online at: www.jgpt.co.in

RESEARCH ARTICLE

Corrosion Protection of Stainless Steel by Electro Polymerization of 4- (2-Hydroxy Benzamido) -4- Oxobut- 2 -Enoicacid and Study its Biological Activity

Sana A. Habeeb, Khulood A. Saleh

Department of chemistry, College of Science, University of Baghdad, Iraq.

Abstract

Poly4-(2-hydroxy benzamido)-4-oxo but-2-enoi cacid (PHOE) was prepared by the electrochemical polymerization of 4-(2-hydroxy benzamido)-4-oxobut-2-enoicacid (HOE) monomer on stainless steel (St.S) asanti -corrosion coating. Atomic Force Microscope (AFM), Fourier transform infrared techniques (FTIR) and cyclic voltammetry were used to characterize the properties and the structure of the polymer layer. The corrosion behavior of uncoated and coated St.S were estimated from Tafels plots using Potentiostatic technique in 0.2 M HCl solution as corrosive environment at temperature range(293 – 323) K. Nanomaterials such as graphene and Nano ZnO in the different concentrations were added to monomer solution to improve the corrosion resistance of St.S surface so that the results showed that the values of corrosion protection efficiency for polymeric coating increase with adding Nanomaterials . In addition the kinetics and thermodynamics parameter were calculated for St.S corrosion before and after polymeric coating in the acidic medium, moreover, the influence of the prepared polymer on some strains of bacteria was studied.

Keyword: *Anti-corrosion, Electrochemical polymerization, Stainless steel, Coating, Antibacterial activity.*

Introduction

Intrinsically conducting polymers e.g poly thiophene, poly pyrrole, poly aniline and their derivatives have attracted great attention in the recent years[1] due to their interesting properties in many technological applications such as sensors [2], batteries [3], dye sensitized solar cells [4] and corrosion protection coatings [5,8].Corrosion Protection by conducting polymer extensively has been investigated recently. because they have wide range of π- electron delocalization along their back bone [9] led to form an electric field on the metal surface to suppress the corrosion reactions by hindering flow of electrons from steel to oxidant [10, 18].

Conducting polymers can be synthesized by electro chemical polymerization technique [19]. It's necessary in this method caring in choosing the electro polymerization conditions specially the current and the applied potential to control the rate of polymerization [20].Conductive polymer that obtained from electro deposition was used to prevent of stainless steel from corrosion in corrosive medium by interact with steel substrate to form a native layer to inhibit corrosion process. Several mechanisms were proposed to synthesize conducting polymer [21] such as barrier protection, corrosion inhibitor, anodic and cathodic protection. in the anodic protection the conducting polymers work as oxidant to the steels lead to form passive oxide film which can shifted the electrode potential to the passive direction [22]. Adding Nano materials to conductive polymers it's one of the interesting researches to improve the protective coating on the metals and alloys against corrosion. These polymers with Nano materials established often offered enhanced electrical, mechanical, and corrosion resistant properties [23].

In this study poly 4-(2-hydroxy benzamido)-4-oxo but-2-enoic acid (PHOE) was prepared by electrochemical polymerization of the monomer (HOE) on St. S surface the characterization of the polymer film(PHOE) was identified by using (AFM), (FTIR) techniques and cyclic voltammetry method. The corrosion behavior of uncoated and coated St. S in acidic solution at different temperature was studied and the biological

effect of adding Nanomaterials (n-ZnO, Graphene) was studied to improve the coating by polymer against corrosion and the effect of the preparing polymer with Nanomaterial coating composite was studied also on strains of bacteria

Experimental

Preparation of the Monomer (HOE)

(0.98g) of maleic anhydride was dissolved in (10ml) of dioxane in the flask at room temperature. Then (1.37g) of salicyl amide was dissolved and added to the flask reaction. The reaction was continued to the 3hour at 25C°. At last the yellow precipitate product was formed, filtered and dried under vacuum .the chemical reaction shown in Scheme 1.

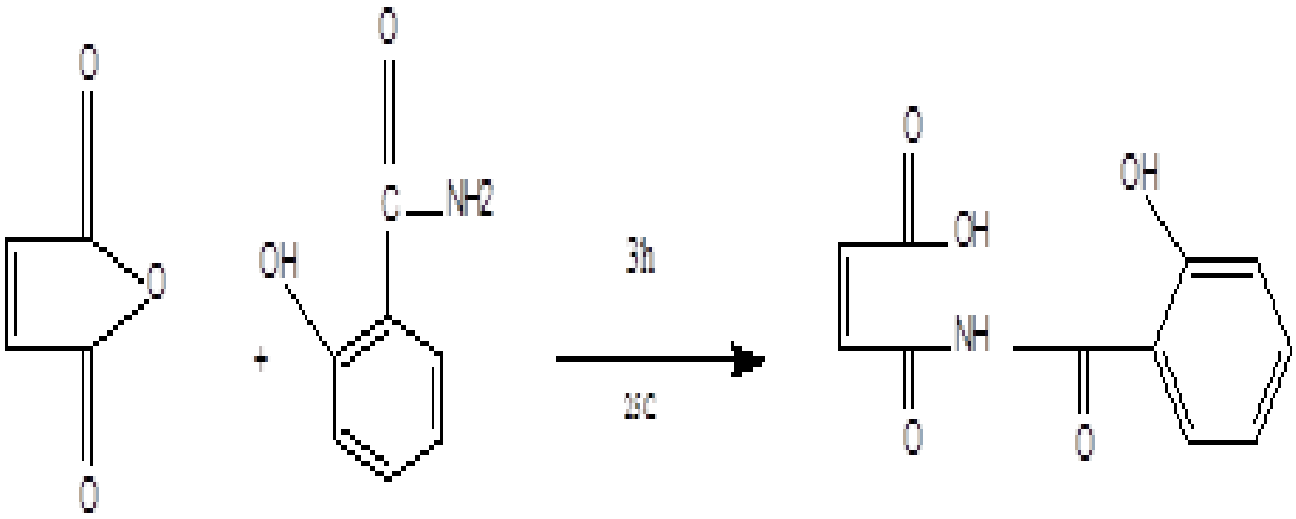

Scheme1: Preparation of the monomer (HOE)

Electro Chemical Polymerization of the Monomer (HOE)

The electrochemical polymerization of (HOE) on the 316 St. S (anodic electrode) surface was accomplished by using a regulated (DC) power supply. The electrodes were cleaned and washed by distilled water then acetone. The solutions which are prepared for the polymerization included dissolve 0.1g of the monomer (HOE) in 100 ml of distilled water with three drops of H2SO4 (95%) concentration as supporting electrolyte [24].

The polymer film was deposited on the anodic surface at 293K. Further 0.004g of graphene was added to the monomer solution after dispersion it also 0.04g of n-Zno was added to the monomer solution to improve the coating film against corrosion and biological activity.

Electro Chemical Corrosion Study

For corrosion study, three-electrodes as cell including a working electrode St.S; coated or non-coated), reference electrode (SCE) and counter or auxiliary electrode (platinum electrode).Anodic and cathodic polarization for the corrosion of (316) St.S was carried out under potentiostatic conditions in 0.2M HCl for coated and uncoated St.S at temperature range (293-323)K.

Electro Deposition of PHOE on St.S by Cyclic Voltammetry

The electrodeposition of PHOE film on St.S electrode has occurred through the electrochemical polymerization of the aqueous solution containing [0.2g monomer (HOE) +200ml distilled water + 3drop of H2SO4 (95%)] by cyclic voltammetry within a potential range from (-2000 to 2000) mv and a scan rate at 40mv/s.

Result and Discussion

The Electro Chemical Cyclic Voltammetry Study of PHOE Coating

The cyclic voltammogram was recorded during the electro deposition of PHOE film on St.S. it was used to investigate the redox properties of the polymeric film. Fig 1 shows the successive cyclic voltammogram obtained with PHOE. From the first scan, an oxidation wave starts at about 1.5v which can be referred to the oxidation of monomer. The intensity of this oxidation wave decreases during the following scans and the oxidation wave shifted to the higher potential which indicates the electropolymerization of monomer. The polymerization rate increases when the potential was higher than 1.5v.

During the reverse potential sweep, the reduction peak appears at 0.6v which can be referred to the reduction of the polymer. This peak decreases in intensity as the polymer coating film grows with a successive scan indicating that the polymer is well grown. At the end of repetitive cycles, a pale brown polymer coating becomes visible.

The increases in the anodic current were referred to electropolymerization of the polymer. But these current decreases gradually with an increasing number of the scan, therefore, the coating film growth during cycling conducted the decrease in current with increasing cycle number [25].

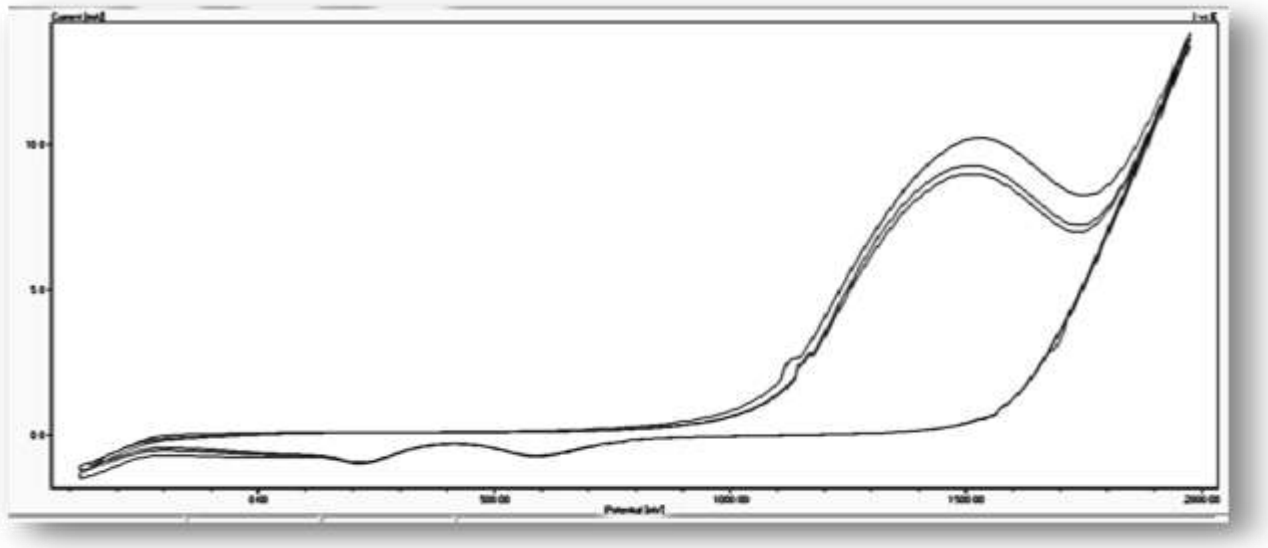

Fig 1: Cyclic voltammogram for electro polymerization of HOE

Mechanism of Polymerization

The electrochemical polymerization reactions for graphting and growth of the (PHOE) film on metal surface were proposed by Cationic [26, 27] or radical mechanism [28, 35]. In the cationic mechanism scheme (2-A) the first step is to transfer the electron from the monomer to the working electrode (metal surface) (A1). This transfer for electron leading to the formation of radical cation adsorbed on the electrode surface which is appeared in (A2).This radical cation can be desorbed and reacted in the solution for giving rise into a component of low molecular weight (A3) Then the (HOE) molecule can be added through the cationic mechanism at the charged end of adsorbed oxidized (HOE) (A4). The radical mechanisms are shown in the Scheme (2-B) [36]. This mechanism proceeds through homolytic scission of the double bond (C=C). The homolytic rupture of the double bond (C=C) is highly improbable considering the initial polarization of the bond which is improved under the field created by an electric double layer [37, 38].

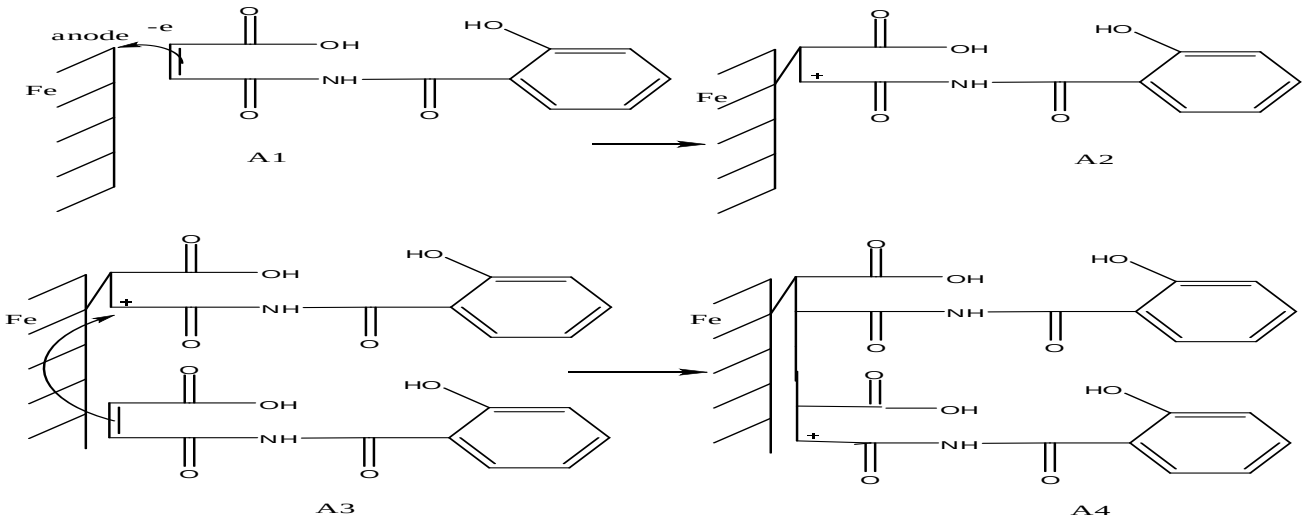

Scheme 2-A Cationic mechanism for the Grafting and the Growth of (PHOE) Films

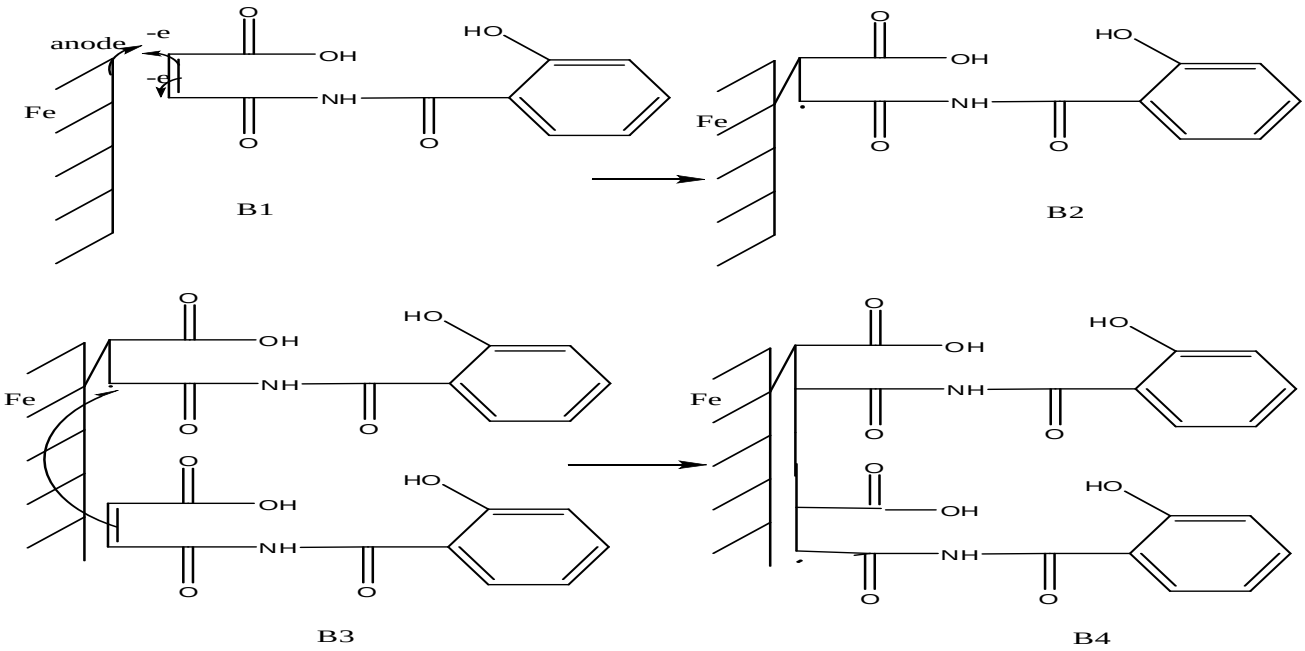

Scheme 2-B: Radical mechanism for the Grafting and the Growth of (PHOE) Films

The Structure of PHOE

FT-IR Analysis

The structure of the polymer (PHOE)) that prepared from the monomer (HOE) by electro chemical polymerization are examined by FT-IR spectroscopy. The spectrum of FT-IR Fig (2A) for the monomer shows that HC=CH olifenic group appeared at 3211cm^{-1}. The transmission peak of C=O carboxylic group appeared at 1699cm-1 ,the peak at 3350cm^{-1} attributed for OH- hydroxyl group, the band of NH- amide group appeared at 3263cm-1, the band of C=O amide group appeared at 1629cm^{-1}, the disappeared of the double bond(C=C) olifenic group in Fig (2B) that confirm the formation of polymer(PHOE).The transmission peak comparatively broad because the polymer (PHOE) has abroad chain distribution [39, 40].

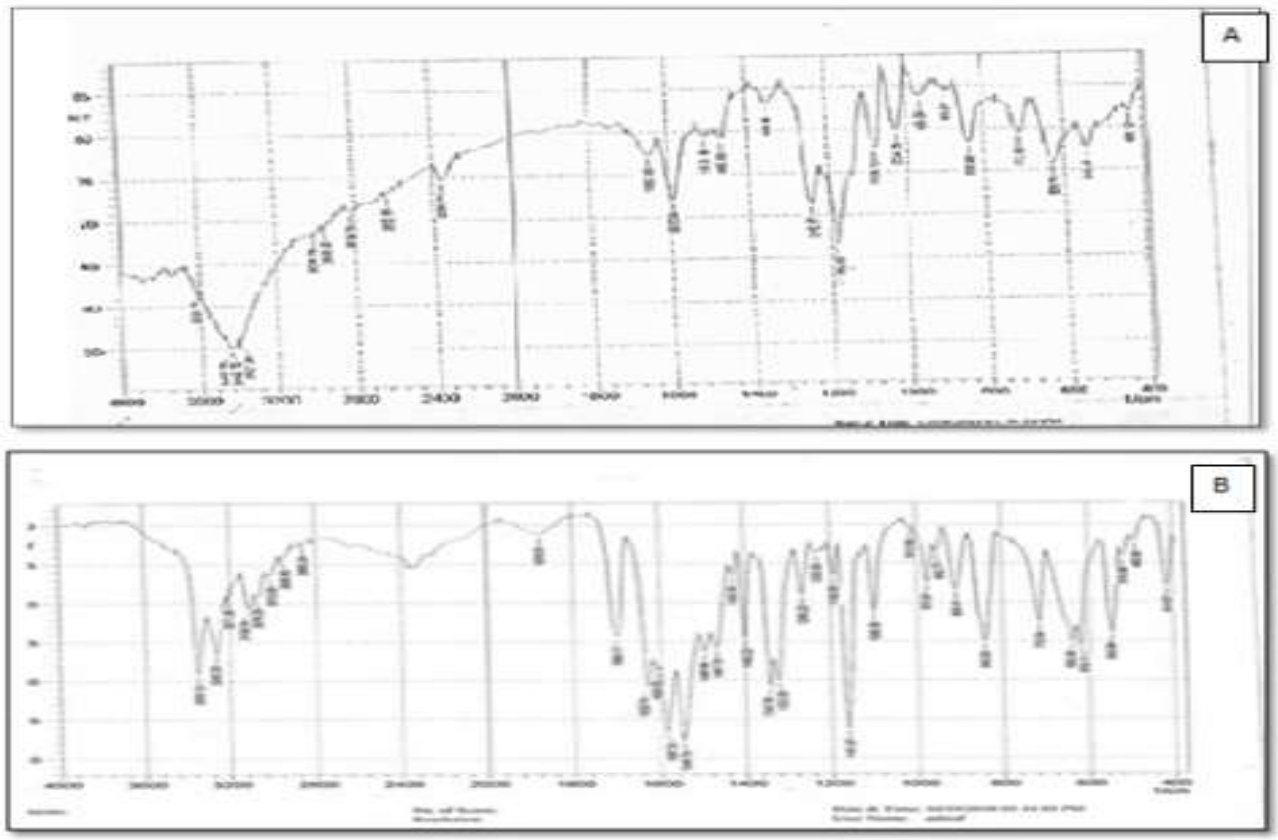

Figure 2: FT-IR for A-the monomer (HOE), B- The polymer (PHOE)

Atomic Force Microscope (AFM)

The surface topography of the St.S coated with (PHOE) in the presence and absence of Nanomaterials (graphene and n-ZnO) was investigated through AFM technique. (Fig.3) show the 3D of the AFM images of all applied coated films. In AFM analysis the diameter of the coated film without Nanomaterial was in average of 123.64nm while the diameter average of a coated film with Graphene reach to 90.73nm and reach to 113.43nm for the coated film with n- ZnO. The results for all applied layers were indicated there was a decrease in the grain size after modification of the polymer with Nanomaterials [41].

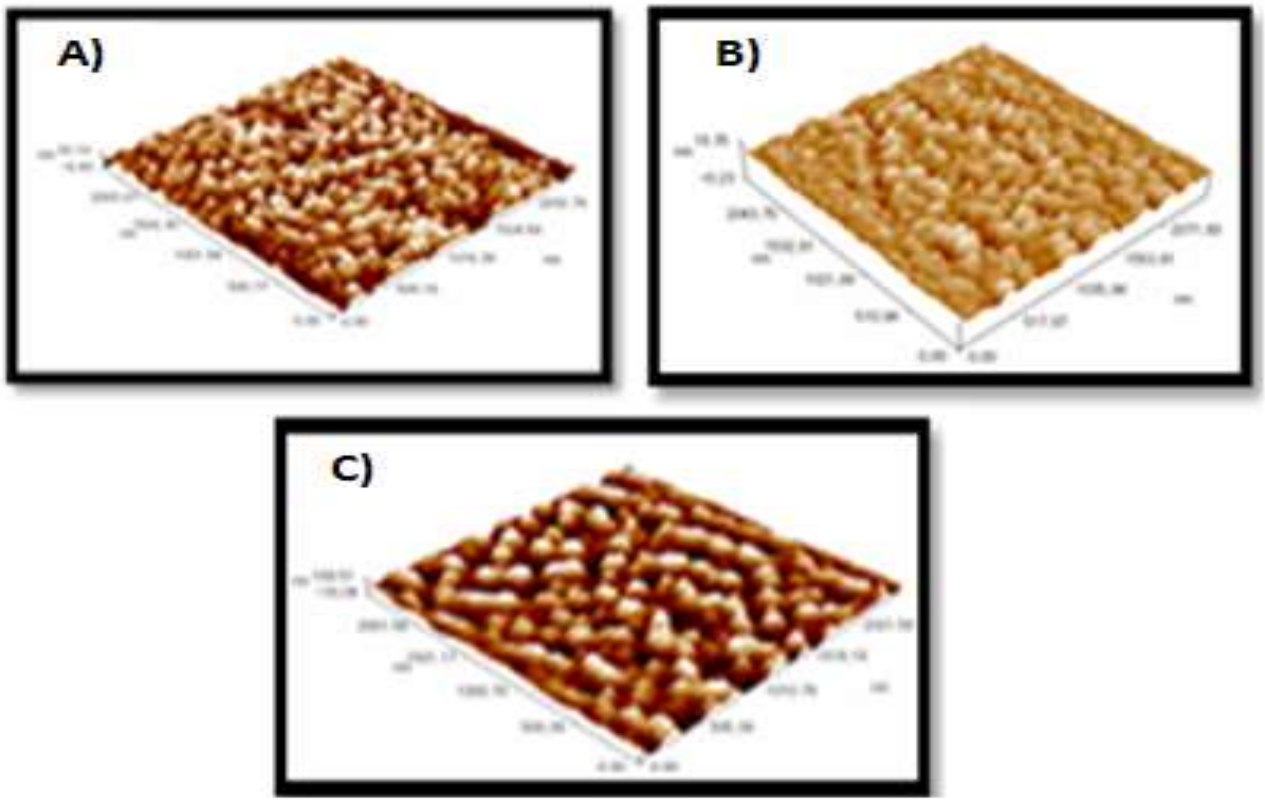

Figure 3: AFM images for A) stainless steel coated PHOE without Nano material , B) stainless steel coated PHOE with Graphene, C) stainless steel coated PHOE with n-ZnO Nano

Potentiostatic Polarization Measurements

The influence of polymeric coating film on the anodic and cathodic polarization curves for the corrosion of St. Sin (0.2) M HCl solution was studied at the temperature range (293 - 323) K. The influence of adding various nanomaterial compound [n-Zno, graphene] for the monomer solution on the corrosion of uncoated and coated St.S by(PHOE)in 0.2MHCl solution is shown in Fig (4) (PHOE) The corrosion current density Icorr was determined by extrapolation of anodic and cathodic Tafel plot and the influence of polymer coating in presence and absence of nanomaterials on the corrosion parameter of the St.S were shown in table 1. This parameter including corrosion current density (Icorr), corrosion potential (Ecorr), anodic Tafel slope (ba) and cathodic Tafel slope (bc), weight loss, penetration loss, polarization resistance (Rp) and protection efficiency (PE %). The polarization resistance (Rp) can be calculated according to the following equation (1) [42].

$$Rp = \frac{ba\,bc}{2.303\,(ba+bc)} Icorr \quad \text{..... (1)}$$

While the protection efficiency (PE %) can be calculated from the equation (2) [43]

$$PE\% = [1 - \frac{Icorr}{Icorr^{\circ}}]\ 100 \text{..... (2)}$$

Where: Icorr°, Icorr is the corrosion rate of uncoated and coated stainless steel respectively.

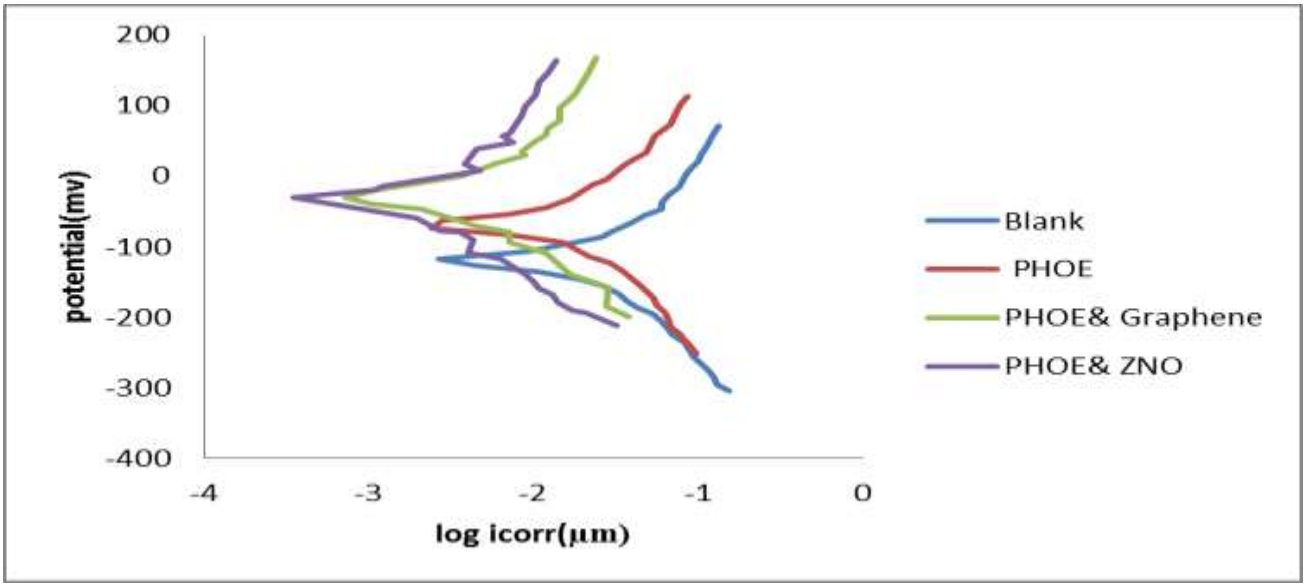

Figure 4: Tafel plot for the corrosion of uncoated stainless steel & coated St.S with PHOEin 0.2MHCl solution at 293K

Table 1: St.S Corrosion parameters in 0.2M HCl with and without coating at different temperature

Coating	T/K	-Ecorr mV	Icorr µA/cm²	- bc mV/Dec	ba mV/Dec	PE%	Weight loss g/m².d	Penetration loss[mm/y]	Rp Ω.cm²
Blank 0.2M HCl	293	116.7	18.42	188.7	159.8	-	1.48	$2x10^{-1}$	2039..681
	303	126	21.37	199.1	185.8	-	1.72	$2.32x10^{-1}$	1952.858
	313	206.6	24.35	207.7	220.5	-	1.96	$2.65x10^{-1}$	1906.821
	323	271.8	25.89	171.6	258.5	-	2.08	$2.82x10^{-1}$	1729.746
PHOE	293	72.1	5.46	73.2	90	70.35	$4.39x10^{-1}$	$5.94x10^{-2}$	3210.309
	303	79.4	7.36	78.5	84.6	65.56	$5.93x10^{-1}$	$8.01x10^{-2}$	2402.228
	313	156	8.92	88.4	95	63.36	$7.18x10^{-1}$	$9.71x10^{-2}$	2229.039
	323	205.6	10.45	85.1	121	59.64	$8.41x10^{-1}$	$1.14x10^{-1}$	2075.997
PHOE & Graphene	293	31.4	1.73	89	84.5	90.608	$1.39x10^{-1}$	$1.88x10^{-2}$	10879.46
	303	51.5	2.41	83.6	85.4	88.722	$1.94x10^{-1}$	$2.62x10^{-2}$	7611.434
	313	92.9	3.15	102.7	99.3	87.064	$2.53x10^{-1}$	$3.42x10^{-2}$	6959.272
	323	187.3	4.61	58.7	104.3	82.194	$3.71x10^{-1}$	$5.01x10^{-2}$	3537.854
PHOE& n-Zno_n	293	38.9	0.91361	93.6	89.1	95.04	$7.35x10^{-2}$	$9.94x10^{-3}$	21695.03
	303	63	1.38	69.6	90.4	93.54	$1.11x10^{-1}$	$1.5x10^{-2}$	12373.27
	313	75.8	4.44	137	200.7	81.76	$3.13x10^{-1}$	$4.23x10^{-2}$	8657.358
	323	181.7	5.41	98.1	106.1	79.103	$4.35x10^{-1}$	$5.88x10^{-2}$	40.91.075

It is clear from table (1) that Ecorr of coated St.S by PHOE has been shifted to more positive values and corrosion current density increases with increasing temperature but its decrease after adding nano materials to the monomer solution which lead to increase the protection effecting for St.S corrosion When the (PHOE) film crafted with Nanomaterial coated on the St.S the Ecorr shifted to the noble direction and the RP values were increased [44]

Kinetic and Thermodynamic of Activation Parameters

The influence of temperature on the corrosion rate of St.S in the presence and absence of different coating by (PHOE) at temperatures from 293 to 323K were studied. The Arrhenius equation (3, 4) was used to calculate the activation energies as shown in Fig (5) [45].

$$C.R = \mathrm{Aexp}(\frac{-\mathrm{Ea}}{\mathrm{RT}})\,]\,100 \quad \ldots\ldots\ldots\ldots\ldots\ldots \textbf{(3)}$$

$$logC.R = \mathrm{logA} - \frac{-\mathrm{Ea}}{2.303\,\mathrm{RT}} \ldots\ldots\ldots\ldots\ldots\ldots \textbf{(4)}$$

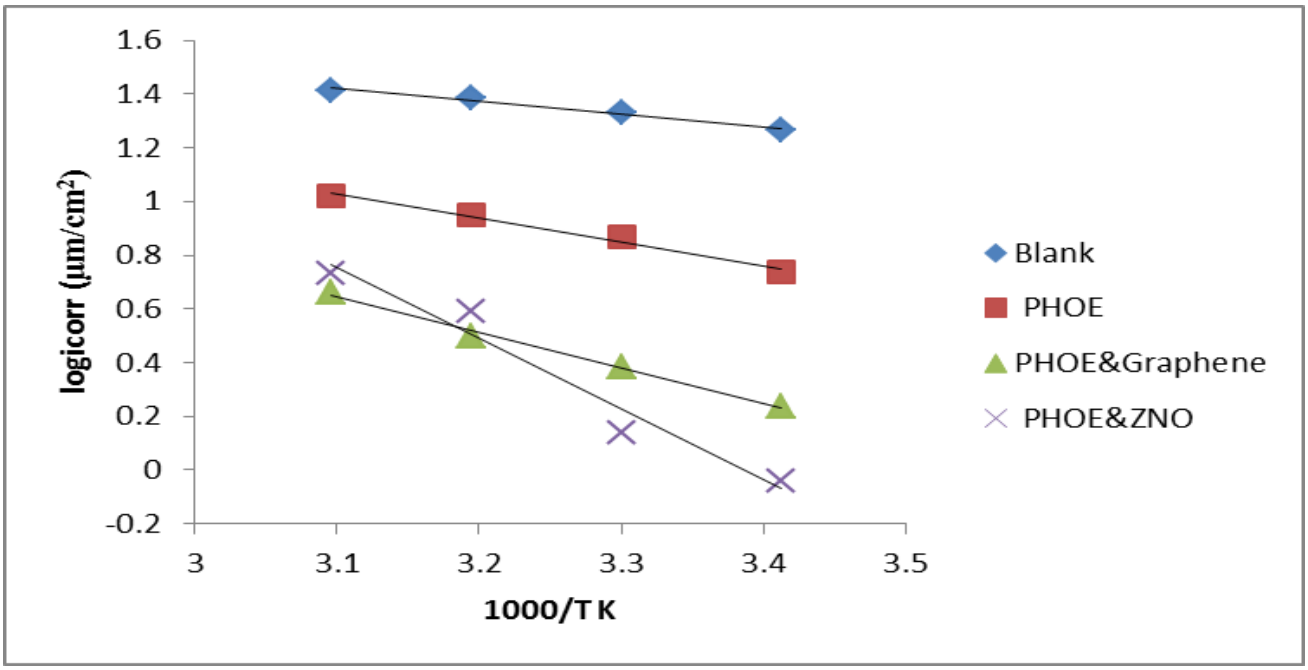

Figure 5: Arrhenius Plot of log icorr versus 1/T for St. S in 0.2 M HCl in the absence and presence coating

The values of the entropy of activation ΔS* and the enthalpy of activation ΔH* for the corrosion of uncoated and coated St.S were estimated from (Fig6) from transition state equation (5, 6).

$$C.R = \frac{RT}{Nh}\exp\left(\frac{\Delta S*}{R}\right)exp(\frac{-\Delta H*}{RT}) \ldots\ldots\ldots\ldots \textbf{(5)}$$

$$(log\frac{C.R}{T}) = log\frac{R}{Nh} + \frac{\Delta S*}{2.303R} - \frac{\Delta H*}{2.303RT} \ldots\ldots\ldots\ldots\ldots \textbf{(6)}$$

While the values of the activation free energy ΔG* was calculated using Gibbs equation (7) [46].

$$\Delta G^* = \Delta H^* - T\Delta S^* \ldots\ldots\ldots\ldots\ldots \textbf{(7)}$$

Where (C.R) is the corrosion rate, (A) the pre-exponential factor, (Ea) is the apparent the activation energy, (T) the absolute temperature, (R) the gas constant (8.314 J mol-1 K-1),(h) Plank's constant (6.626176 x 10-34JS), (N) is Avogadro's number (6.022 x 1023 mol-1), (ΔS*) the entropy of activation, (ΔH*) the enthalpy of activation and (ΔG*) the Gibbs free energy.

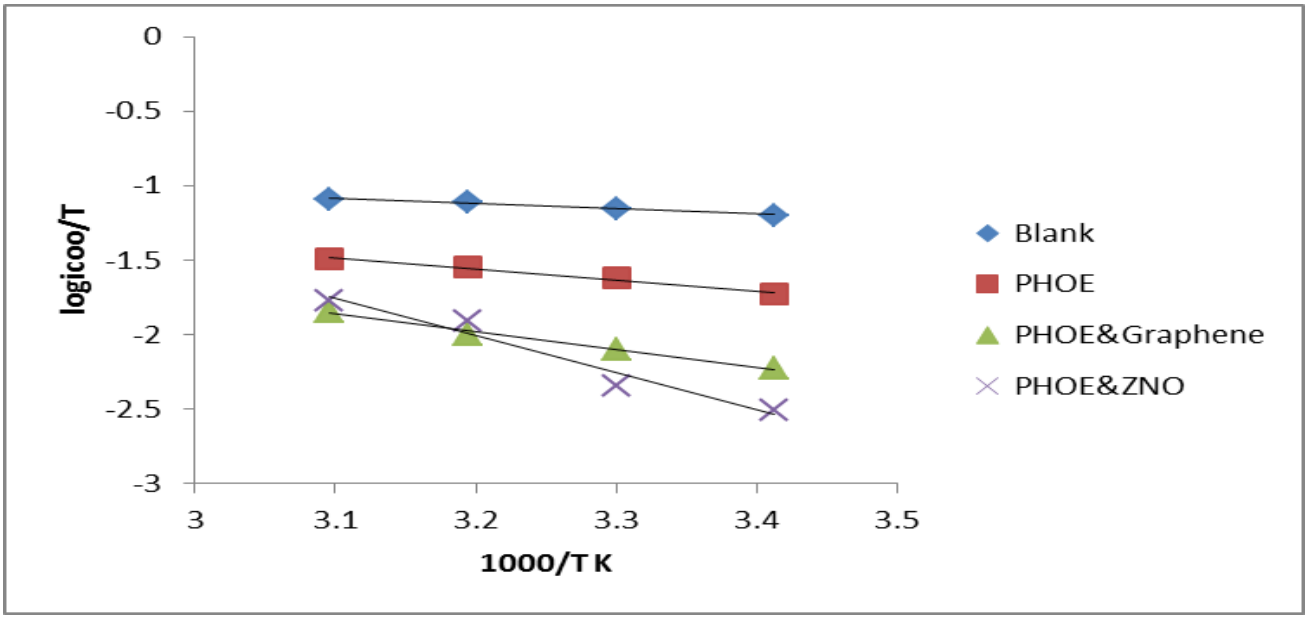

Figure 6: Arrhenius Plot of log i corr/T versus 1/T for St.S corrosion in 0.2 M HCl in the absence and presence coating.

Table 2: Activation parameters Ea, ΔH*, ΔS* and ΔG* for uncoated and coated St. S dissolution in 0.2 M HCl

Coating	R^2	Ea kJ.mol^{-1}	A/Molecule. Cm^{-2}.S^{-1}	R^2	ΔH* KJ. K^{-1}. mol^{-1}	-ΔS* J .K^{-1}. mol^{-1}	ΔG KJ. K^{-1}. mol^{-1}
Blank HCl 0.2M	0.9789	9.1026	$4.721*10^{26}$	0.9580	6.5464	198.1117	64.593
							66.574
							68.555
							70.536
PHOE	0.9854	16.8993	$34.885x10^{26}$	0.9792	14.343124	181.48056	67.517
							69.332
							71.147
							72.961
PHOE & Graphene	0.993	25.2072	$31.999x10^{27}$	0.9916	22.64915	163.051438	70.423
							72.054
							73.684
							75.315
PHOE & Zno	0.958	50.1502	$44.755x10^{31}$	0.9536	47.59405	83.67313	72.110
							72.947
							73.770
							74.620

All the calculated kinetic and thermodynamic parameters values were represented in Table (2), the results show that the activation energies in the presence of (PHOE) film were increased indicates the higher protection efficiency resulted by coating. The values of activation energies increase with adding different nanomaterials in which coating indicating increasing in the energy barrier of the corrosion reaction.

The positive sign of the activation enthalpies (ΔH*) for coated and uncoated St.S indicates to endothermic nature of transition state reaction of St.S. The values of ΔS* for the uncoated and coated ss are negative. Means that the activation complex in the rate determining step representing association rather than dissociation step. Indicating that a decrease in disordering takes place on going from reactant to the activated complex [47, 48].

The positive values of ΔG* recorded in a Table (2) showed almost small change with the rise in temperature and indicating non-spontaneous nature of transition state for uncoated and coated St.S.

Antibacterial Activity

Polymeric coatings are diversified use in most Pharmaceutical and biomedical applications and sectors. The polymeric coating gives a redoubt of functionalities for

their implicit hosts In the area of biological activity, The results of antibacterial activity of polymer with and without nanomaterial are listed in Table (3). The result indicates that the polymer with and without nanomaterial compounds possess moderate activity against Escherichia coli and Staphylococcus aureus [49].

Table 3: Antibacterial activity of the test polymer and polymer nanomaterial

Compound	*Escherichia Coli*	*Staphylococcus aureus*
PHOE	**13**	**15**
PHOE & Graphene	**15**	**18**
PHOE & n-Zno	**17**	**18**
Amoxcillin	**30**	**30**

Solvent DMSO: [C]: 800 µg/ml

Conclusion

The electrochemical polymerization of HOE on St.S was found to be a good protective coating in 0.2 M HCl solution. The protection efficiency of polymer PHOE increases with adding Nanomaterials to monomer solution exceptionally with n-ZnO and decreases with temperature increase (293-323) K.

The corrosion potential of PHOE coating acted as anodic type inhibitor in 0.2MHCl. The values of activation energies increase with adding different nanomaterials in which coating indicating increasing in the energy barrier of the corrosion reaction. The positive sign of the activation enthalpies (ΔH*) for uncoated and coated St.S indicate to endothermic nature of transition state reaction of St.S.

The values of ΔS * for the uncoated and coated ss are negative. This means that the activation complex in the rate determining step representing association rather than dissociation step. Indicating that a decrease in disordering takes place ongoing from reactant to the activated complex. The positive values of ΔG*was recorded show almost small change with the rise in temperature and indicating the non-spontaneous nature of transition state for uncoated and coated St.S.

The AFM analysis for PHBAOBEA with and without Nanomaterials(Graphene, ZnO) shows the grains size for polymer decrease after modification with nanomaterials also the results of Antibacterial activity was showed that the polymer with and without nanomaterial compounds possess moderate activity against Escherichia coli and Staphylococcus aureus.

References

1. Simon P, Gogotsi Y (2008) Nature materials, 7 (11): 845-8542.
2. RM Rosa, RL Szulc, RWC Li (2005) J. Gruber, Macromol. Symp., 229: 138.
3. HK Song, G Palmore, R Tayhas (2006) Adv. Mater., 18: 1764.
4. Q Qin, J Tao, Y Yang (2010) Synth. Met., 160: 11-67.
5. Olad A, Nosrati R (2013) "Preparation and corrosion resistance of nanostructured PVC/ZnO–polyaniline hybrid coating," Progress in Organic Coatings, 76: 113-118.
6. Olad A, Naseri B (2010) "Preparation, characterization and anticorrosive properties of a novel polyaniline/clinoptilolite nanocomposite," Progress in Organic Coatings, 67: 233-2389.
7. Mahulikar PP, Jadhav RS, Hundiwale DG (2011)"Performance of Polyaniline/TiO2 Nanocomposites in Epoxy for Corrosion Resistant Coatings," Iranian Polymer Journal, 20: 367-376.
8. Khalil SK, Khulood AS, Muna IK (2018) Novel Electro Polymerization Method to Synthesized Anti-corrosion Coated Layer on Stainless Steel Surface from (N-Benzothiazolyl Maleamic Acid) and Study its Biological Activity International Journal of Pharmaceutical Quality Assurance, 9(3): 253-259.
9. M Manickavasagam, K Zeya Karthik, M Paramasivam, SV Iyer (2002) 473-494.

10. Deshpande PP, Jadhav NG, Gelling VJ, Sazou D (2014) Conducting polymers for corrosion protection: a review. J. Coat. Technol. Res, 11.

11. Nwankwo HU, Olasunkanmi LO, Ebenso (2017) E. E. Experimental, quantum chemical and molecular dynamic simulations studies on the corrosion inhibition of mild steel by some carbazole derivatives. Sci. Rep, 7: 24-36.

12. Sheng Q et al (2017) Simultaneous hydrate and corrosion inhibition with modifed poly(vinyl caprolactam) polymers. Energy Fuels, 31: 6724-6731.

13. Singer F, Schlesak M, Mebert C, Hön S, Virtanen S (2015) Corrosion properties of polydopamine coatings formed in one-step immersion process on magnesium. ACS Appl. Mater. Interfaces, 7: 26758-26766

14. Lutz A et al (2015) A shape-recovery polymer coating for the corrosion protection of metallic surfaces. ACS Appl. Mater. Interfaces, 7: 175-183.

15. Wang Y et al (2015) Self-immunity microcapsules for corrosion protection of steel bar in reinforced concrete. Sci. Rep. 5: 18484.

16. Xia, W. et al (2016) Functionalized graphene serving as free radical scavenger and corrosion protection in gamma-irradiated epoxy composites. Carbon, 101: 315-323.

17. Krishnamurthy, A. et.al (2015) Superiority of graphene over polymer coatings for prevention of microbially induced corrosion. Sci. Rep., 5: 13858.

18. Wu Y, Zhao W, Wang W, Wang L, Xue Q (2017) Novel anodic oxide flm with self-sealing layer showing excellent corrosion resistance. Sci. Rep., 7: 13-44.

19. PP Deshpande, NG Jadhav, VJ Gelling, D Sazou (2014) Conducting polymers for corrosion protection: a review, J. Coat. Technol. Res., 11: 473-494

20. Ormecon Chemie, GmbH Co, KG Kornkamp (1998) Dispersion as the link between basic research and commercial applications of conductive polymers (polyaniline) B. Wessling/ Synhetic Metals, 93: 143-15434.

21. Khan MI, Chaudhry AU, Hashim S, Zahoor MK, Iqbal MZ (2010) Chem. Eng. Res. Bulletin, 14 (2):73-86

22. Lacoa I, Cadena F, Liesa F Prog (2005) Org. Coat., 52: 151-160.

23. Gangopadhyay R, De A (2000) Chem. Mater. , 12, 608. [29] William, S. H.Jr. and Richard, E. O." Preparation of graphitic ox-ide". Journal of American Chemical Society, 80: 1339-1394. 1958. https://doi.org/10.1021/ja01539a017

24. William SH Jr, Richard EO (1958)" Preparation of graphitic ox-ide". Journal of American Chemical Society, 80: 1339-1394. https://doi.org/10.1021/ja01539a017

25. Deepak Kumarappa, ariyanayagam (2011) Advance delectrodematerials for electrochemical super capacitors, M.Sc., mc master university, materials science and engineering.

26. Leonard-Stibbe E, Viel P, Younang E, Defranceschi M, Lecayon G, Delhalle J (1992) Grafting and Growing of Poly (N-Vinyl-2-Pyrrolidone) Films on a Platinum Anode: Experimental and Theoretical Study, In Polymer-Solid Interfaces, 93-104.

27. Younang E, Léonard-Stibbe E, Viel P, Defranceschi M, Lécayon G, Delhalle J (1992) Prospective theoretical and experimental study towards electrochemically grafted poly (N-vinyl-2-pyrrolidone) films on metallic surfaces, Molec. Engin., 1(4): 317-233.

28. Léonard-Stibbe E, Lécayon G, Deniau G, Viel P, Defranceschi M, Legeay G, Delhalle J (1994) The cationic polymerization of N-vinyl-2-pyrrolidone initiated electrochemically by anodic polarization on a Pt surface, J. Polym. Sci.: Part A, Polym. Chem., 32(8): 1551-1555.

29. Jerome R, Mertens M, Martinot (1995) On The Electrochemical Polymerization of Acrylonitrile and N-Vinylpyrrolidone - New Insight into the Mechanism, L. Adv. Mater., 7(9): 807-809.

30. Beamson G, Briggs D (1992) High Resolution XPS of Organic Polymers, John Wiley & Sons: Chichester, 192.

31. Ivanov DV, Yelon (1996) Chemical-Sensitivity of the Thickness-Shear-Mode

Quartz-Resonator Nanobalance, A. J. Electrochem. Soc., 143(9): 2835-2841.

32. Czerwinski WK, Makromol (1991) Solvent effects on free-radical polymerization, 2.† IR and NMR spectroscopic analysis of monomer mixtures of methyl methacrylate and N-vinyl-2-pyrrolidone in bulk and in model solvents, Chem., 192(6):1297-1305.

33. Landis WR, Perrine (1968) Nuclear Magnetic Resonance and Infrared Spectroscopic Study of NVinyl Compounds, T. D. Appl. Spectrosc., 22(3):161-164.

34. Lin-Vien D, Colthup NB, Fateley WG, Grasselli JG (1991) The Handbook of Infrared and Raman Characteristic Frequencies of Organic Molecules, Academic: San Diego, 74.

35. Mertens M, Calberg C, Martinot L, Jerome R (1996) The Electro reduction of Acrylonitrile - A New Insight into the Mechanism, Macromolecules, 29(14):4910-4918.

36. Haaf F, Sanner A, Straub F (1985) Polymers of NVinylpyrrolidone: Synthesis, Characterization and Uses, Polymer J., 17(1):143 -152.

37. Raynaud M, Reynaud C, Ellinger Y, Hennico G, .Geskin VM, Lazzaroni R, Mertens M, Jerome, Delhalle J (1990) High Electric-Field Effects on the Acrylonitrile Molecule - an Abinitio Study, J. Chem. Phys., 142(2): 191-201.

38. R Bredas, JL (1996) Acrylonitrile on Cu (100): A density functional theoretical studyof adsorption and- electrochemical grafting, J. Chem. Phys., 105(8): 3278-328.

39. Silverstein RM, Webster FX, Kiemle DJ (1963) Spectrometric Identification of Organic Compounds, 7th ed., John Wiley & Sons, Westford, US.

40. Shirner R, Fuson R, Cartin D, Mrril T (1980) The systematic identification of organic compound, 8th ed., John Wiley & Sons, New York.

41. P. Karthikeyan M, Malathy R Rajavel (2016) Poly(ophenylenediaminecoaniline)/ZnO coated on passivated low nickel stainless steel Journal of Science: Advanced Materials and Devices, 1-7.

42. Bardal E (2004) Corrosion and protection. Springer, 1-44.

43. Abdel Aal MS, Radwan S, El-Saied A (1983) Phenothiazines as corrosion inhibitors for zinc in NH4Cl solution, Brit. Corros. J, 18(2):102-1069.

44. Anthony SSR, Susai R (2012) Inhibition of corrosion of carbon steel in well water by arginineZn2+ system, J. Electrochem. Sci. Eng. 2(2): 91-104.

45. Umorena SA, Obota IB, Ebensob EE, ObiEgbedib NO (2009) The Inhibition of aluminium corrosion in hydrochloric acid solution by exudate gum from Raphia hookeri, Desalination, 247(1-3): 561-572.

46. Mars G Fontana, Norbert D Greene (1984)" Corrosion Engineering", 2rd ed. (McGraw-Hill, NY, 297-304

47. Abdallah M (2002) Rhodanine azosulpha drugs as corrosion inhibitors for corrosion of 304 stainless steel in hydrochloric acid solution, Corros. Sci., 44(4): 717-728.

48. Noor EA, Al-Moubaraki AH (2008) Thermodynamic study of metal corrosion and inhibitor adsorption processes in mild steel/1-methyl-4[4(-X) - styryl pyridinium iodides/hydrochloric acid systems, Mater. Chem. Phys., 110 (1):145-154.

49. Roselli M, Finamore A, Garaguso I, Britti MS, Mengheri E (2003) Zinc oxide protects cultured enterocytes from the damage induced by E. coli. J. Nutr., 133(12): 4077-4082.

